Complexities of the Thermal Boundary Conditions when Testing Timber using the Fire Propagation Apparatus

Cuevas J.I.[1,] *, Hidalgo J.P.[1], Torero J.L.[2], Maluk C.[1]

[1] *University of Queensland, Brisbane, Australia*
[2] *University of Maryland, College Park MD, USA*
**Corresponding author's email: j.cuevas@uq.edu.au*

ABSTRACT

The potential for Engineered Timber Products to self-extinguish is the focus of study of numerous researchers worldwide, but regardless of scientific efforts, a relatively high discrepancy still exists on the definition of the critical threshold for self-extinguish. This discrepancy can be attributed to the variability in the test sample material, testing conditions, and/or test methodologies executed. The work presented herein analyses the impact of the thermal boundary conditions imposed by the experimental setup, analysing the divergence of the thermal response from the idealized scenario usually proposed in theoretical frameworks. In particular, the impact of two key assumptions, a semi-infinite solid behaviour and the existence of one-dimensional heat transfer within the solid, are evaluated by means of a case study corresponding to a series of bench-mark experiments conducted in the Fire Propagation Apparatus. By means of a simple one-dimensional heat transfer model, it was found that in order to guarantee a semi-infinite solid behaviour for a thermal exposure of 50kW/m^2 during one hour, a minimum sample thickness of 150 mm is needed. Furthermore, the results of this numerical model have shown that imposing an adiabatic boundary condition in the back face of the sample decreases the time during which this assumption can be sustained, whereas having an exposed or heat sink boundary condition at the back face generates the opposite effect. Following, in order to assess the validity of assuming a one-dimensional heat transfer regime during the tests, the radiative heat transfer between the heating elements and the sample was simulated. The results show the presence of additional heat fluxes through the lateral faces of the sample. The effectiveness of insulating the lateral faces of the sample, to minimize this undesired effect, was analysed by means of a set of experimental tests. The results show that the effect of the lateral incident heat flux over the sample can be minimized, but not discarded. Thus, it is not valid to assume a one-dimensional heat transfer regime within the solid. It is proposed that neglecting these effects can, therefore, cause an inaccurate determination of the thermal conditions imposed during testing.

KEYWORDS: heat transfer, timber, fire propagation apparatus, bench-scale testing.

INTRODUCTION

The timber industry has experienced a renaissance in the built environment. Driven by the increasing need for eco-friendly construction and by the vast potential of engineered timber products, there has been a rapid growth in the design and construction of timber structures. Materials like Cross-laminated Timber (CLT), Laminated Vernier Lumber (LVL), and Glue-laminated Timber (Glulam) stand as comparable alternatives to conventional construction materials such as concrete or steel. The equivalence (and sometimes advantage) of engineered timber is not only associated with load-bearing capacity, but also with a range of other considerations: cost, ease of construction, aesthetics, energy saving, and many others.

Regarding fire safety, a number of regulations incorporate fire safety guidelines for the design of load-bearing timber structures; mainly by means of fire rated encapsulation. Nevertheless, driven by

Proceedings of the Ninth International Seminar on Fire and Explosion Hazards (ISFEH9), pp. 959-969
Edited by Snegirev A., Liu N.A., Tamanini F., Bradley D., Molkov V., and Chaumeix N.
Published by Saint-Petersburg Polytechnic University Press
ISBN: 978-5-7422-6498-9 DOI: 10.18720/spbpu/2/k19-88

the aesthetic aspect of timber, there is an increasing demand for timber to remain exposed; hence, vulnerable to the effects of direct exposure to fire. This presents a challenge that must be addressed before timber can be used with the same confidence we use other building materials and systems [1, 2].

The challenge of achieving fire-safe timber structures is not new; in the early 40s, the work presented by Hottel [3] concluded that a minimum incident radiant heat flux of about 32 kW/m^2 was necessary to sustain flaming combustion of small-scale spruce test samples. Also, Bamford et al. [4] reported that flame extinction of deal panels occurred immediately after the external source of heat was halted and the critical mass loss rate of the sample was approximately 2.5 g/m^{2}s. In the late 70s, Tewarson and Pion [5], and Petrella [6] formally validated the fundamental principle that the heat transferred from the flame impinging on the timber surface is not sufficient to sustain flaming combustion. This led to state that an external source of heat was required to sustain timber combustion.

More recently, Inghelbrecht [7] reported that the occurrence of self-extinguishment is always attained for small-scale Cross-Laminated Timber (CLT) Radiata Pine samples after removing the external source of heat. In this work, the time to self-extinguishment varied because of heat-induced delamination of the lamellae of the CLT samples. For the samples that did not experience delamination, a critical mass loss rate of 4 g/m^{2}s was registered when flame extinction occurred. Considering a more rigorous definition, Crielaard et al. [8] performed a series of bench-scale CLT samples and determined a critical incident radiant heat flux of 5-6 kW/m^2 for the complete stop of combustion (flaming and smouldering). Emberley et al. [9], also testing bench-scale CLT samples, determined a critical mass loss rate of 4.0 g/m^{2}s and critical incident radiant heat flux of 42 kW/m^2, for the cease of flaming combustion. Bartlett et al. [10] tested bench-scale CLT samples and concluded that the conditions for flame extinction occur at approximately 32 kW/m2 and a mass loss rate of 3.5 g/m^{2}s. Based on the numerous studies done to date, a relatively high discrepancy still exists on the definition of self-extinguishment of timber and the critical threshold for its occurrence.

As presented above, the broad range of configurations and methodologies used to study self-extinguishment of timber generates a high degree of discrepancy and uncertainties in the results obtained. As a result, inefficient design criteria are obtained. For example, a difference of a 30% on the critical incident radiant heat flux for self-extinguishment (considering values of 42 and 32 kW/m^2) can be translated into under- or over-sized CLT lamellae, decreasing the level of safety in the first case, and increasing production costs in the second. Furthermore, the inconsistencies among the results obtained at different scales of study prevent the formulation of guidelines that responsibly ensure the fire-safe use of engineered timber in load-bearing structures.

The work described herein aims at tackling the inconsistencies associated with the study of self-extinguishment of timber and the testing methods used for this, by developing a series of testing guidelines that homogenise the analysis of self-extinguishment at a bench-scale, and more specifically when using FM Global's Fire Propagation Apparatus (FPA). The work is divided into two stages: modelling and experimental.

METHODOLOGY

Theoretical Background

When timber is exposed to heat, the exposed surface will gradually heat up and influenced by the thickness of the test sample and the species of the wood, temperature in-depth will increase. Furthermore, a physicochemical degradation process will be triggered because of this temperature increase. This degradation includes moisture evaporation, generation of pyrolysis gases, char formation and oxidation, and as a result of the regression of the exposed surface [11, 12]. Figure 1a

presents a schematic of some of the processes involved in the heating and flaming combustion of timber.

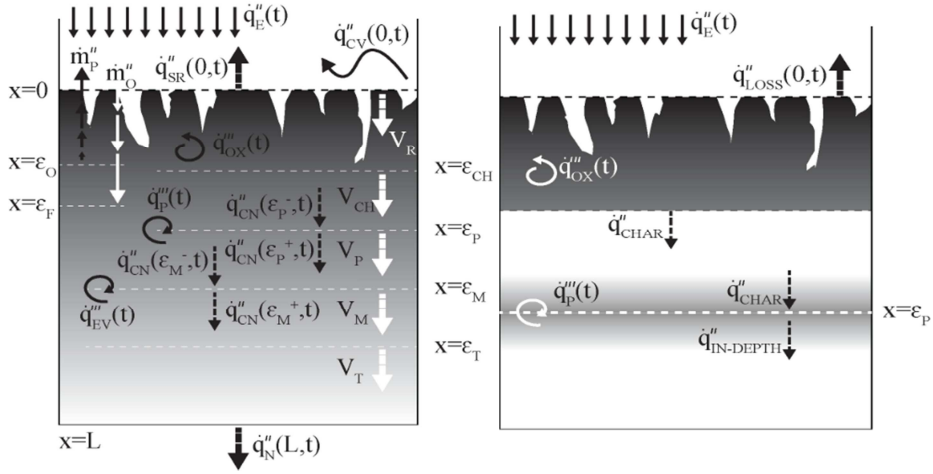

Fig. 1. Different heat fluxes and processes occurring during the burning of timber. (a) Complete scenario, adapted from [11]; (b) Simplified scenario proposed by Emberley et al. [13].

Due to the intrinsic difficulties that arise when dealing with this problem, it is often common to simplify this model by means of the following assumptions:

1. One-dimensional heat transfer is considered.
2. The sample is assumed to behave as a semi-infinite solid.
3. The effects of cracks the material's porosity [14], moisture migration [15], and surface regression at the exposed surface are neglected.
4. Only the material's thermal conductivity is considered as temperature-dependent.
5. Pyrolysis is considered as an isothermal process happening at an infinitely fast rate at a temperature of T_{pyr}. Consequently, the progression of the pyrolysis front can be described by tracking the T_{pyr} isotherm within the solid.

Under these assumptions, Emberley et al. [9] proposed the following energy balance on the charring front:

$$\rho_{char} c_{p\,char} \frac{\partial T}{\partial t} = \dot{q}''_e + \dot{q}''_{oxi} - \dot{q}''_{char} - \dot{q}''_{loss}\,, \tag{1}$$

where $\dot{q}''_e$ is the incident heat flux at the exposed surface of the char layer and it incorporates the heat flux provided by the flame and the one from external sources. The term $\dot{q}''_{oxi}$ represents the energy added due to the exothermic oxidation reaction, and the term $\dot{q}''_{loss}$ represents the energy losses. Following, the rate of energy transferred from the char layer into the pyrolysis front $\dot{q}''_{in-depth}$ is evaluated by means of the following equation,

$$\dot{q}''_{in-depth} - \left(-k \left. \frac{\partial T}{\partial x} \right|_{x=\varepsilon_P} \right) = \Delta H_p \dot{m}''_f\,, \tag{2}$$

where ΔH_p is the heat of pyrolysis and $\dot{m}_f^{"}$ is the mass flow of pyrolysis gases being generated. Thus, combining these two last expressions, the following expression is obtained, that allows relating the mass flow of gases consumed in the flame with the different heat fluxes involved in the process:

$$\dot{m}_f'' = \frac{1}{\Delta H_p}\left(\dot{q}_e'' + \dot{q}_{oxi}'' - \dot{q}_{loss}'' - \left(-k \left.\frac{\partial T}{\partial x}\right|_{x=\varepsilon_P} \right) - \rho_{char} c_{p\,char} \frac{\partial T}{\partial t} \right) \tag{3}$$

From this expression, self-extinguishment can be evaluated through worst-case scenario analysis; the maximum burning rate achievable (that translates into the maximum flow of pyrolysis gases $\dot{m}_f^{"*}$) is obtained when the subtracting terms in the right side are minimized and steady-state conditions are reached. If self-extinguishment is achieved for $\dot{m}_f^{"*}$, it will be achieved for every other mass flow smaller than this one.

PROPOSED APPROACH

From the theoretical formulation presented above, the experimental determination of a $\dot{m}_f''$ only becomes valid if the assumptions used in the theoretical framework are met. The two most powerful and common assumptions made in this study are (1) that test sample exhibits a semi-infinite solid behaviour, and (2) that it experiences a dominant one-dimensional heat transfer in the direction transversal to the exposed surface.

In order to quantify the impact of the first assumption, a one-dimensional transient heat transfer model was implemented. The model considered the heat diffusion equation presented in Eq. 4, with a uniform heat flux boundary condition on the exposed surface (Eq. 5):

$$\frac{\partial k}{\partial T}\left(\frac{\partial T}{\partial x}\right)^2 + k\frac{\partial^2 T}{\partial x^2} = \rho c_p \frac{\partial T}{\partial t}, \tag{4}$$

$$-\left.\frac{\partial T}{\partial x}\right|_{x=0^+} = \dot{q}_e'' - \dot{q}_{loss}'' = \dot{q}_e'' - h_T\left(T_S - T_\infty\right), \tag{5}$$

where $\dot{q}_e''$ is the total incident heat flux over the exposed surface, and the heat losses term $\dot{q}_{loss}''$ is defined by means of a total heat transfer coefficient h_T, evaluated as presented in Eq. 6, according to Hidalgo [16]:

$$h_T = 0.0761\left(T_S\right) + 9.5761 \tag{6}$$

Where T_S is the temperature of the exposed surface, in Celsius. In particular, this model aimed at (1) determining the minimum sample thickness that ensures a semi-infinite behaviour, and (2) due to the spatial limitations of the experimental setup, the determined sample thickness may not be feasible. Thus, the effect of the back-face boundary condition needs to be quantified. This was done by simulating three possible scenarios:

- Insulated (adiabatic) back face, described by a Neumann boundary condition:

$$-k\frac{\partial T\left(L,t\right)}{\partial x} = 0 \tag{7}$$

- Exposed back face, described as

$$-k\frac{\partial T(L,t)}{\partial x}=h\left(T_{\infty}-T(L,t)\right). \tag{8}$$

- Heat sink attached to the back face, described according to Carvel et al. [17] as

$$-k\frac{\partial T(L,t)}{\partial x}=\frac{1}{A}\left(\frac{\partial T}{\partial t}mc_p\right)_{HS} \tag{9}$$

Where m and c_p are the mass and specific heat of the heat sink. For the thermal properties of timber, a moving-boundary model for a non-reacting solid was implemented. This model considered three different phases (wet timber, dry timber, and char) and was implemented following the approach proposed by Lautenberger and Fernandez-Pello [18], in which the solid's density is assumed constant for each phase, while the thermal conductivity and specific heat capacity vary according to the temperature, as presented in the following expressions:

$$k(T)=k^{*}\left(T/T_r\right)^{n_k} \tag{10}$$

$$c_p(T)=c_p^{*}\left(T/T_r\right)^{n_c} \tag{11}$$

Where T_r is a reference temperature, k^{*} and c_p^{*} are referential values of the solid's conductivity and specific heat capacity (evaluated at T_r) and the exponents n_k and n_{cp} describe the variation of these properties according to the element's temperature. The corresponding values used to evaluate these parameters can be found in [19].

Following, a comparison was made in order to determine which one of these scenarios resembles the most to the ideal one (semi-infinite solid). This comparison was based on the in-depth temperature profiles and the progression of the thermal wave for each one of the scenarios.

In order to ensure one-dimensional heat transfer, the thermal boundary conditions under which the samples are tested were characterized and quantified. With this information, the need of additional measures (such as insulating the sides of the sample) was determined, and their effectiveness (based on how much the testing conditions resemble the one-dimensional scenario) analysed.

Experimental setup

The bench-scale experiments were conducted in the Fire Propagation Apparatus (FPA) developed by FM Global, under the specifications of the ASTM E2058-13a standard [20].

Figure 2 presents a schematic of the test apparatus. The upper portion of the calorimeter corresponds to an exhaust system that collects all the combustion-generated products that are driven to the gas analyser. This exhaust system is composed by an intake funnel, a test section where gas temperature and exhaust flow rate are measured, and a high-temperature sampling outlet from where samples of the gases are sent to the gas analyser.

The lower part of the calorimeter corresponds to the combustion chamber which comprises a combustion air distribution chamber, sample holder, weighing cell, ignition device (ethylene pilot flame), and four infrared heaters. In order to evaluate the sample's mass loss, a Tedea Huntleigh Load Cell was used. To characterize the thermal response of the sample, a set of type K thermocouples embedded into the sample and connected to a National Instruments NI-9210 data acquisition system was used.

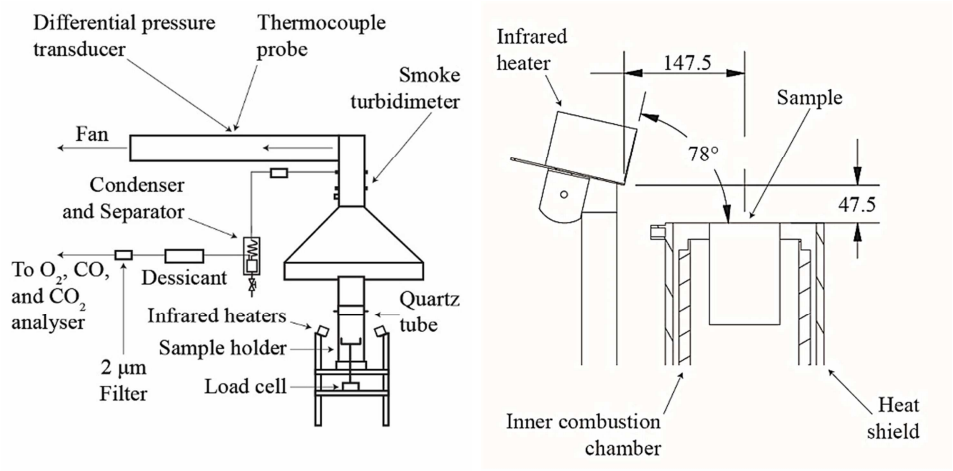

(a) (b)

Fig. 2. Schematic of the experimental apparatus. (a) General schematic of the calorimeter; (b) Geometrical configuration of the infrared heaters (all dimensions in mm).

RESULTS AND DISCUSSION

Semi-infinite solid behaviour assumption

As previously mentioned, to determine the impact of the semi-infinite solid hypothesis, a numerical one-dimensional heat transfer model was implemented under the parameters presented in Table 1, and solved by means of an implicit finite-difference scheme [21, 22] ($O(\Delta t, \Delta x^2)$, and taking Δt = 5 ms, Δx = 0.25 mm). The model was validated by replicating the results presented in [19], were the same material thermal properties were used. A thermal exposure of 50kW/m^2 during one hour was selected. Furthermore, this thermal exposure is imposed in order to match a set of experiments conducted by the author and not reported here.

Table 1. Numerical simulation parameters

Parameter	Value
Thermal exposure	50 kW/m^2 during 3600 s
Material	White pine (*Pinus sp.,* thermal properties from [18])
Dimensions	Rectangular prism with a cross-section of 90x90 mm and variable length

Figure 3a shows the modelled in-depth temperature profiles of a timber, for different times. As it can be seen, the moisture evaporation front (based on the 100 ºC isotherm) reaches a depth of 50 mm after approximately 2650 s, almost 45 minutes. For that same time, the pyrolysis front (based on the 385 ºC isotherm according to [18]) has progressed to approximately 10 mm of depth. Furthermore, if an increase of 0.5 ºC in the original temperature is defined as the criterion to track the progress of the thermal wave (minimal resolution available in the experimental set-up, given by the thermocouple's uncertainty), it was found that the thermal wave has propagated through the sample up to a depth of 150 mm. Therefore, this sample thickness is presented as a candidate for the optimal sample thickness.

Following, the next step was to determine the effect and relevance of the boundary condition at the unexposed face (located at 150 mm from the exposed surface). The results of this stage are presented in Figure 3b. From the figure, it can be seen that the thermal behaviour of the solid is

almost independent of the boundary condition considered at the unexposed surface, except for the later portion of it. It was found that the heat sink (in a larger level) and exposed surface (in a lower level) boundary conditions overestimate the arrival of the thermal wave when compared to the semi-infinite wave propagation curve. On the other hand, the adiabatic back boundary condition was found to underestimate the time of arrival of the thermal wave when compared to the same parameter. These results can be explained by the following reasons; an adiabatic boundary has a barrier effect on the propagation of heat, therefore facilitating the storage of it within the element and finally elevating its temperature. For the other two conditions, their effect is the complete opposite; if the element's back face is exposed to the ambient (modelled as air at a constant temperature of 18°C) or to an adjacent heat sink (modelled as a 20 mm thick Aluminium block), there is an additional heat flux at this boundary, evacuating (by means of convection/radiation or conduction, respectively) any amount of heat that reaches this portion of the sample, allowing it to remain cooler for a longer period.

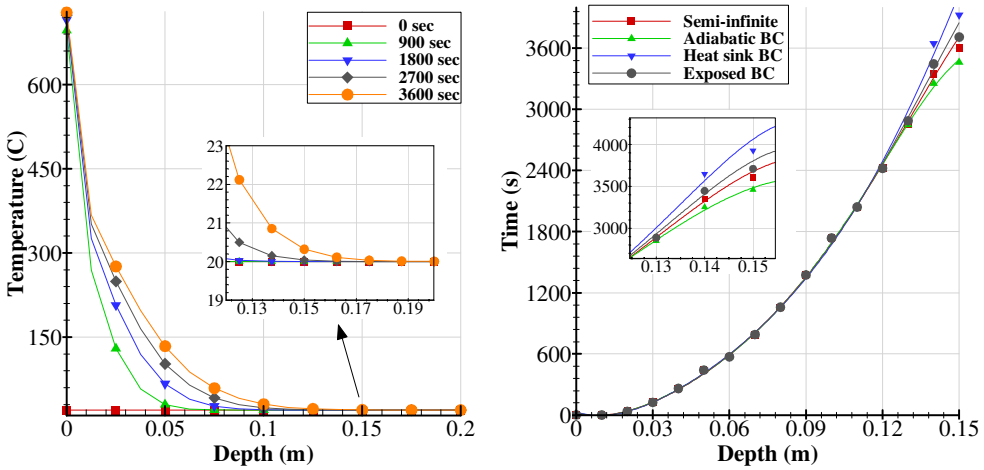

Fig. 3. Thermal response of the modelled timber element. (a) In-depth temperature profiles for different times; (b) Time needed for the thermal wave to reach a certain depth, for different boundary conditions at the unexposed surface.

From this first part of the study, it can be partially concluded that a timber sample of 150 mm thick with a heat sink element attached to its unexposed face it is expected to show a semi-infinite solid behaviour when exposed to a constant incident heat flux of 50 kW/m^2.

ONE-DIMENSIONAL HEAT TRANSFER ASSUMPTION

For the next part of the present study, a set of experimental tests were conducted to determine the boundary conditions under which the samples are actually tested in the experimental setup described previously. One of the most relevant parameters in this point is to characterize the radiant incident heat flux over the exposed surface of the sample. This characterization was done by means of a numerical model that simulated the radiant incident heat flux over the sample. This model was calibrated using a set of experimental measurements conducted using a Medtherm Schmidt-Boelter-type heat flux gage (model: GTW-10SB-8-36-40-484). The results of the model are presented in Fig. 4.

From Fig. 4a, it can be seen that the heater's configuration imposes over the exposed surface an incident heat flux over sufficiently homogeneous to partially enable the one-dimensional heat transfer assumption, as discussed Boulet et al. [23]. On the other hand, Figure 4b indicates the

presence of an unneglectable (approx. 40% of the maximum heat flux) heat flux over the lateral faces of the element. To completely validate the one-dimensional transfer assumption, it is necessary to mitigate the effect of this lateral heating by means of corrective actions. Figure 4c shows the data used to calibrate this model. In the figure, the black dots represent the 17 measurements points considered in the calibration. An overall agreement can be seen between the data collected experimentally (Fig. 4c) and the results obtained by the model (Fig. 4a).

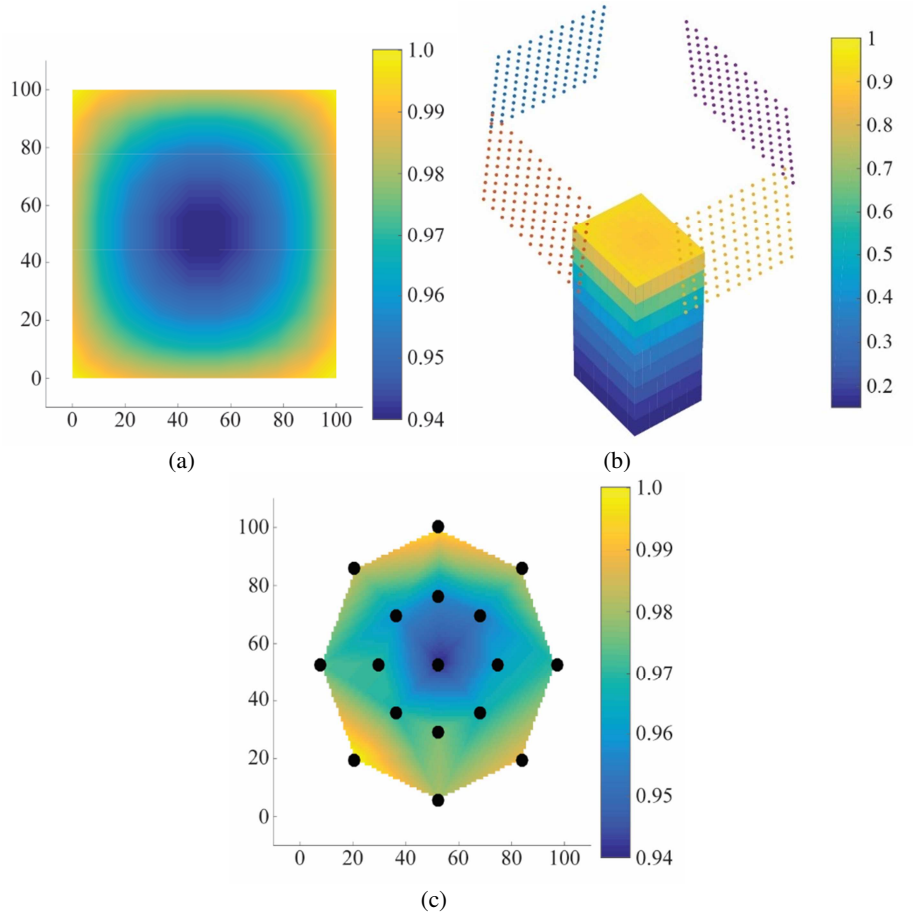

Fig. 4. Results of the numerical modelling of the incidental heat flux over the sample (all units in mm). (a) Normalized spatial distribution of the incident heat flux over the complete sample; (b) Normalized spatial distribution of the incident heat flux over the exposed surface. (c) Results of the experimental measurements used to calibrate the numerical model.

The effectiveness of a corrective action consisting on protecting the sides of the sample with an insulating jacket was evaluated by means of an experimental study which compared the thermal degradation of samples (in terms of mass loss and in-depth temperature measurements) with and without insulation. A general description of this experimental campaign is presented in Table 2 and the results in Fig. 5.

From Figs. 5 a and b, the relevance of the presence of lateral insulation is left in evidence; the temperature curves registered by the thermocouples placed at 35 mm from the exposed surface show temperature difference of approximately 150 °C after 900 s. Moreover, the heating profile described by the unprotected sample at a depth of 75 mm is with the range of the one showed at 55 mm by the protected sample for the majority of the exposure time. This radical difference in the

thermal behaviour of the sample is also evidenced when looking at the thermal profiles presented in Fig. 5c; after 900 s the unprotected sample has lost approximately 40% of its original mass, while the protected on has lost approximately 10% of it.

Table 2. Parameters for the experimental campaign

Parameter	Value
Thermal exposure	50 kW/m^2 (constant), during 15 min
Sample dimensions	Rectangular prism with an exposed surface of 90x90 mm, 150 mm thick
Material	Cross-laminated Timber (Radiata Pine)
Sample preparation	(1) Inner layer of 9 mm thick Ceramic Paper (SiO_2-Al_2O_3 based material); (2) Outer lining of reflective material
Thermocouples	12 Type K thermocouples (TC) in-depth placed at: 35 mm (4 TCs), 55 mm (2 TCs), 75 mm (2 TCs), 95 mm (1 TC) mm centred about the sample. 3 TCs at a depth of 95mm within the insulation (inner, middle, and outer)

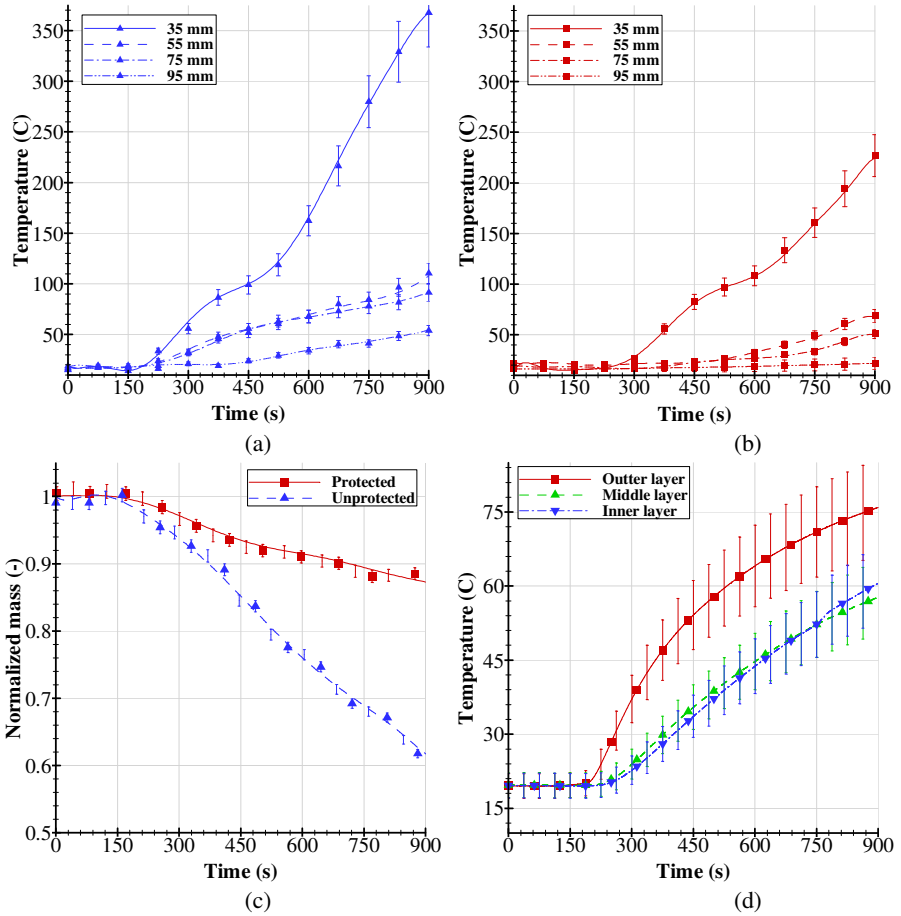

Fig. 1: Experimental evaluation of the effectiveness of lateral insulation. (a) In-depth temperature profiles for an unprotected sample; (b) In-depth temperature profiles for a protected sample; (c) Comparison of mass loss measurements; (d) Temperature profiles within the insulation, at a depth of 95 mm from the exposed surface of the test sample.

Regardless of the improvement in the thermal response of the sample due to the presence of lateral insulation, this corrective action is not sufficient to ensure one-dimensional heat transfer, as presented in Fig. 5d. The measurements shown in Fig. 5d correspond to the readings of the thermocouples positioned at a depth of 95 mm from the exposed surface, within the three insulation layers. The inner layer thermocouple was placed between the inner Aluminium lining (place at the sides of the test sample) and the first layer of Ceramic Paper, the middle layer thermocouple was placed in between the first two insulation layers, and the outer layer thermocouple was placed in between the last two insulation layers. From the figure, it can be seen that the temperature that the insulation reaches is higher than the one at the centre of the sample (at the same depth from the exposed surface). The presence of such high temperatures in the inner insulating layer indicates the heating of the sides of the samples during testing.

CONCLUSIONS

The present work has analysed the relevance of two of the most common assumptions used in scientific analysis experimental bench-scale timber fire studies; the semi-infinite solid behaviour and one-dimensional heat transfer within the solid sample. Meeting these assumptions in bench-scale testing is not only relevant to achieve results that are consistent with the theoretical frameworks, but also enables the scaling up of these results in order to predict the full-scale fire behaviour of timber. In an attempt to evaluate the conditions necessary to meet these assumptions, a minimum sample thickness was determined by means of a numerical heat transfer model. Following, the unavoidable presence of lateral heating was also identified by simulating the radiative heat transfer between the infrared heaters and the test sample. Furthermore, experimental results show that for a thermal exposure of 50 kW/m^2, after the first 15 minutes (900 seconds) of heating, an unprotected sample will lose up to 30% more mass than a protected sample. Also, results show that temperatures at a depth of 35 mm from the exposed surface can be more than 100°C higher when comparing unprotected and protected test samples. Regarding this last aspect, even though protecting the sides of the sample shifts the thermal response of the element towards an ideal behaviour (i.e. without lateral heating), the protection used within the scope of this work demonstrated not to be sufficient to achieve one-dimensional heat transfer during the full duration of a test.

The presence of heating at the sides of the test sample is given by the need to use a standardized apparatus to perform standardized tests, using non-standardized test samples [20]. Neglecting this effect can, therefore, cause an inaccurate determination of the thermal conditions imposed during testing. This could explain the apparent discrepancy that exists in the determination of the critical conditions for the self-extinction of timber; especially between Inghelbrecht [7], Crielaard et al. [8], Emberley et al. [9], and Bartlett et al. [10].

Finally, in order to generate valuable scientific outcomes, the common theoretical frameworks must be modified to take into account the abovementioned conditions associated with fire testing of timber using the Fire Propagation Apparatus.

REFERENCES

[1] A. Law, A. Bartlett, R. Hadden, N. Butterworth, The Challenges and Opportunities for Fire Safety in Tall Timber Construction, in: 2nd Int. Tall Build. Fire Saf. Conf. 2014, 2014: pp. 17–19.

[2] R. Gerard, D. Barber, A. Wolski, Fire safety challenges of tall wood buildings, National Fire Protection Research Foundation, 2013.

[3] H.C. Hottel, G. Wilkes, Wood Flammability Under Various Conditions of Irradiation, OSRD Publ. 432 (1942).

[4] C.H. Bamford, J. Crank, D.H. Malan, A.H. Wilson, The combustion of wood. Part I, Math. Proc. Cambridge Philos. Soc. 42 (1945) 166–182.

[5] A. Tewarson, R.F. Pion, Flammability of plastics-I. Burning intensity, Combust. Flame 26 (1976) 85–103.

[6] R. V. Petrella, The Mass Burning Rate and Mass Transfer Number of Selected Polymers, Wood, and Organic Liquids, Polym. Plast. Technol. Eng. 13 (1979) 83–103.

[7] A. Inghelbrecht, Evaluation of the burning behaviour of wood products in the context of structural fire design, International Master of Science in Fire Safety Engineering MSc, The University of Queensland, Ghent University, 2014.

[8] R. Crielaard, J.-W.W.G. van de Kuilen, K.C. Terwel, G.J.P. Ravenshorst, P. Steenbakkers, A. Breunese, A. Breunesse, Self-extinguishment of cross-laminated timber, in: Proc. World Conf. Timber Eng. (WCTE 2016), Vienna, Austria, 2016.

[9] R. Emberley, A. Inghelbrecht, Z. Yu, J.L. Torero, Self-extinction of timber, Proc. Combust. Inst. 36 (2017) 3055–3062.

[10] A. Bartlett, R. Hadden, L. Bisby, B. Lane, Auto-extinction of engineered timber: the application of firepoint theory, in: Interflam, 2016.

[11] J.L. Torero, Flaming Ignition of Solid Fuels, in: SFPE Handb. Fire Prot. Eng., 5th ed., Springer New York, 2016: pp. 633–661.

[12] D. Drysdale, An introduction to fire dynamics : 3rd ed., Wiley, Chichester, West Sussex, 2011.

[13] R. Emberley, T. Do, J. Yim, J.L. Torero, Critical heat flux and mass loss rate for extinction of flaming combustion of timber, Fire Saf. J. 91 (2017) 252–258.

[14] R.K.K. Yuen, G.H. Yeoh, G. de Vahl Davis, E. Leonardi, Modelling the pyrolysis of wet wood – I. Three-dimensional formulation and analysis, Int. J. Heat Mass Transf. 50 (2007) 4371–4386.

[15] R. Aseeva, B. Serkov, A. Sivenkov, Fire Behavior and Fire Protection in Timber Buildings, Springer, 2014.

[16] J.P. Hidalgo-Medina, Performance-based methodology for the fire safe design of insulation materials in energy efficient buildings, The University of Edinburgh, 2015.

[17] R. Carvel, T. Steinhaus, G. Rein, J.L. Torero, Determination of the flammability properties of polymeric materials: A novel method, Polym. Degrad. Stab. 96 (2011) 314–319.

[18] C. Lautenberger, C. Fernandez-Pello, A model for the oxidative pyrolysis of wood, Combust. Flame 156 (2009) 1503–1513.

[19] A.F. Osorio, J.P. Hidalgo, P.D. Evans, Enhancing the fire performance of engineered mass timber and its implications to the fire safety strategy, in: Proc. World Conf. Timber Eng. (WCTE 2018), Seoul, Republic of Korea, 2018.

[20] ASTM International, ASTM E2058-13a Standard Test Methods for Measurement of Material Flammability Using a Fire Propagation Apparatus (FPA), i (2013) 30.

[21] T.L. Bergman, F.P. Incropera, D.P. DeWitt, A.S. Lavine, Fundamentals of Heat and Mass Transfer, 7th ed, John Wiley & Sons, 2011.

[22] R.H. Pletcher, J.C. Tannehill, D.A. Anderson, Computational fluid mechanics and heat transfer, 3rd ed., CRC Press, 2013.

[23] P. Boulet, G. Parent, Z. Acem, A. Collin, M. Försth, N. Bal, G. Rein, J.L. Torero, Radiation emission from a heating coil or a halogen lamp on a semitransparent sample, Int. J. Therm. Sci. 77 (2014) 223–232.